Available online at www.sciencedirect.com
ScienceDirect
Tetrahedron 63 (2007) 12629–12638
Tetrahedron

Synthesis and structural properties of porphyrin analogues of bacteriochlorophyll *c*

Marcin Ptaszek, Zhen Yao, Dhanalekshmi Savithri, Paul D. Boyle and Jonathan S. Lindsey*

Department of Chemistry, North Carolina State University, Raleigh, NC 27695-8204, USA

Received 2 August 2007; revised 2 October 2007; accepted 3 October 2007
Available online 7 October 2007

Abstract—The self-assembling photosynthetic pigment bacteriochlorophyll *c* contains α-hydroxyethyl and keto groups on opposite sides of the macrocycle. A porphyrin has been synthesized that contains a 3-hydroxymethyl group and a 15-ethoxycarbonyl group (**ZnP2-OH**). X-ray analysis of **ZnP2-OH** and the related porphyrin containing 5-hydroxymethyl and 15-ethoxycarbonyl groups (**ZnP1-OH**) in each case revealed infinite coordination polymers wherein the zinc porphyrins are bound by Zn–O coordination and are cofacially offset in a staircase architecture.

1. Introduction

Photosynthetic antenna complexes consisting of chlorophylls or bacteriochlorophylls absorb light and funnel excitation energy to the reaction centers.[1] In plants and purple bacteria, the chlorophylls and bacteriochlorophylls are associated with pigment-binding proteins in elaborate 3-dimensional structures. On the other hand, in green photosynthetic bacteria, the bacteriochlorophyll pigments self-associate to give green bodies (i.e., chlorosomes) with little proteinaceous scaffolding.[2] The self-assembly process yields a highly organized molecular architecture that allows efficient collection of light and subsequent energy transfer. Bacteriochlorophyll *c*, a bacterial photosynthetic pigment that readily undergoes self-assembly to yield a functional light-harvesting apparatus, differs only slightly in structure from the plant photosynthetic pigment chlorophyll *a* (Chart 1).[3]

A model for the molecular interactions underlying the self-assembly of the key light-harvesting pigment in green bacteria, bacteriochlorophyll *c*, is shown in Figure 1. The proposed model was developed largely by spectroscopic examination of the 'aggregation' of bacteriochlorophyll *c* and analogues in hydrophobic organic solvents.[2,4] The self-assembly relies on the intermolecular interaction of three key moieties: 3^1-hydroxyalkyl group, central magnesium ion, and 13-keto group; the resulting architecture exhibits partial overlap of the π clouds of the macrocycles.

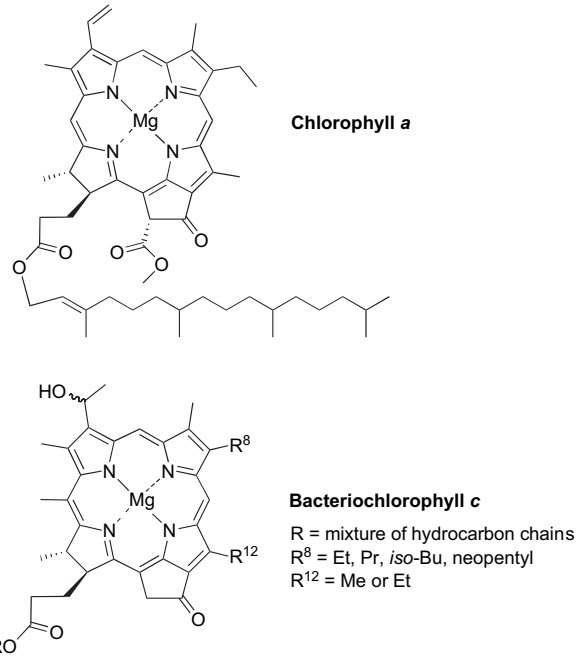

Chart 1.

In the early 1990s, Holzwarth in conjunction with Tamiaki and Balaban began using synthetic approaches to more expansively address the question of 'what substituents at the perimeter of the bacteriochlorophyll molecule are essential to cause the self-assembly process?'[5,6]

Tamiaki has employed semisynthesis of naturally occurring analogues to probe the role of each structural element. The

Keywords: Porphyrin; Self-assembly; Crystal; Photosynthesis; Light-harvesting.
* Corresponding author. Tel.: +1 9195156406; fax: +1 9195132830; e-mail: jlindsey@ncsu.edu

0040–4020/$ - see front matter © 2007 Elsevier Ltd. All rights reserved.
doi:10.1016/j.tet.2007.10.023

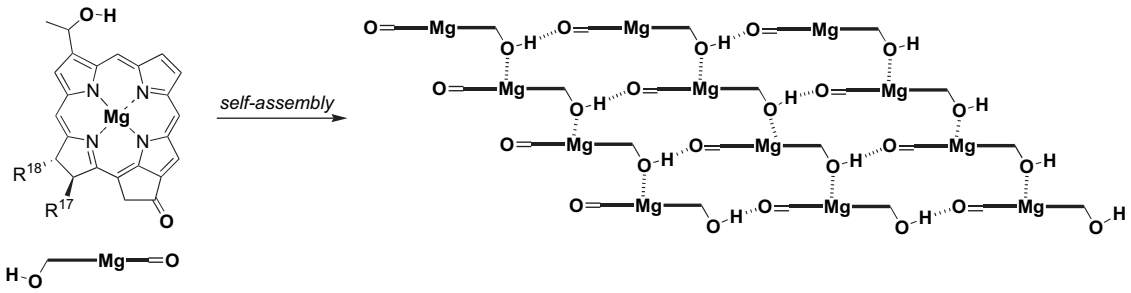

Figure 1. Proposed molecular interactions in the self-assembly of bacteriochlorophyll *c* (selected substituents omitted for clarity).

results of this seminal and comprehensive work have established the extent to which structural variation can be accommodated within the bacteriochlorophyll framework while still maintaining a self-assembly process.[7–41] Balaban has taken a complementary approach that entails the de novo synthesis of porphyrins and chlorins as candidates for analogous self-assembly processes.[42–45] One result of this pioneering work is porphyrin **I**, which contains a 5-(α-hydroxy)ethyl group, 15-acetyl group, and 10,20-bis(3,5-di-*tert*-butylphenyl) groups (Chart 2). Porphyrin **I** crystallizes to give infinite coordination polymers wherein the porphyrins are organized by apical coordination into a staircase architecture.[45] More extensive studies of the self-assembly process can profit from efficient synthetic access to porphyrinic analogues bearing a range of one-carbon substituents. One-carbon substituents appear to be essential; indeed, extensive exploratory work by Balaban revealed that tetraarylporphyrins bearing such substituents at the *p*-positions of the aryl rings did not give the desired assembly process.[42] The results of these approaches have been reviewed in part.[46–49] A wide variety of other substituted porphyrins, particularly with heterocyclic substituents (e.g., imidazole, pyridyl), have been prepared and examined for self-assembly to give larger architectures.[50] The products of most such self-assembly processes have been examined in solution rather than crystals.

Synthetic porphyrins bearing one-carbon substituents are known; however, the syntheses often rely on statistical approaches when two such substituents are required in different oxidation states, as is the case for **I**. The most common procedure at present to access such porphyrins is to introduce two identical substituents (e.g., diformyl, diacetyl) followed by statistical conversion of one group to another one-carbon unit (e.g., hydroxymethyl, carboxy, oxime).[51] Recently we developed methodology for the synthesis of porphyrins bearing from one to four hydroxymethyl groups attached directly to the *meso*-positions.[51] This methodology allowed introduction of hydroxymethyl group(s) together with other one-carbon oxygenic substituents such as ethoxycarbonyl or formyl. However, the synthesis of porphyrins bearing distinct one-carbon oxygenic substituents simultaneously at the *meso*- and β-position remains a challenge.

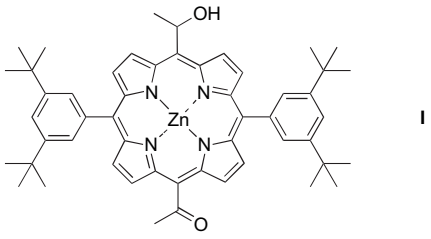

I

Chart 2.

The current methodologies for preparing porphyrins with one β-substituent include (1) the condensation of an aldehyde and a mixture of pyrrole and a β-substituted pyrrole,[52] and (2) the derivatization at one β-position following porphyrin formation.[53,54] Both methods rely on statistical reactions, in turn requiring the desired product to be isolated from a mixture of porphyrins. Although high yields have been reported for introduction of a single deactivating substituent, β-derivatization is typically limited to porphyrins that bear the same substituent at all four *meso*-positions because a statistical reaction will afford regioisomers when a porphyrin carries different *meso*-substituents. Moreover, β-derivatization typically is not applicable for porphyrins with free *meso*-positions due to possible *meso*-substitution.

A key building block in a directed synthesis of a β-substituted porphyrin is the corresponding 3-substituted dipyrromethane. The synthesis of a 3-aryldipyrromethane from a β-aryl-β′-ethoxycarbonylpyrrole and an *N*-protected pyrrole[55] or from an *N*-protected 2-hydroxymethyl-3-arylpyrrole and pyrrole[56] have been reported. A 3,7-dibromoporphyrin was synthesized from a 1,9-diacyl-3,7-dibromodipyrromethane followed by Stille coupling to introduce vinyl groups to the corresponding 3,7-positions of the porphyrin.[57] The β-bromoporphyrin is an attractive platform because a wide variety of substituents can be introduced via Pd coupling reactions.

We previously described the synthesis of a porphyrin that bears a 5-hydroxymethyl group and a 15-ethoxycarbonyl group (**ZnP1-OH**, Chart 3).[51] In this paper, we describe our studies concerning the synthesis of a zinc porphyrin that bears a 3-hydroxymethyl group and a 15-ethoxycarbonyl group (**ZnP2-OH**). (We note that the 3,15-positions should formally be named the 2,10-positions, but we employ the 3,15-descriptor for ease of comparison with **ZnP1-OH** and bacteriochlorophyll *c*.) The synthetic route relies on the preparation of a 3-bromoporphyrin. The crystal packing pattern of **ZnP1-OH** and **ZnP2-OH** are compared with each other and with the known properties of Balaban's porphyrin **I**. Taken together, this work provides information concerning the design of self-assembling crystalline architectures of porphyrins.

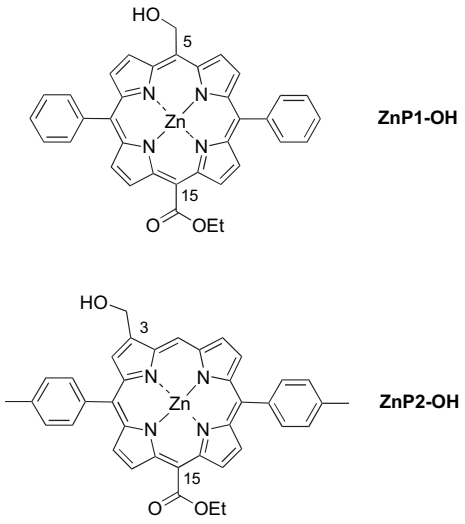

Chart 3.

2. Results and discussion

2.1. Synthesis of porphyrin ZnP2-OH

The synthesis of a 3-bromoporphyrin (**H_2P2-Br**) relied on the availability of 1,9-di-*p*-toluoyldipyrromethane–tin complex **1**.[58] The acyl groups at the 1- and 9-position direct electrophilic bromination to the 3- and 7-position.[57,59] Bromination of **1** with 1 mol equiv of Br_2 yielded the corresponding 3,7-dibromo compound as the major product. On the other hand, treatment of **1** with 1 mol equiv of NBS at −78 °C yielded a mixture of the desired 3-bromo-1,9-diacyldipyrromethane–tin complex **2**, the dibromo product and the starting material in a ratio of 10:1:1.5 as determined by ^{1}H NMR analysis of the reaction mixture (Scheme 1). Compound **2** was isolated by chromatography in 62% yield. The regiochemistry of bromo substitution was established by NOESY spectroscopy. While the bromination does not afford a single product, the desired 1,9-diacyldipyrromethane bearing a single 3-bromo substituent was readily isolated. The dialkyltin complex affords a relatively hydrophobic, highly soluble compound that is readily handled. In general, conducting the separation following bromination of the 1,9-diacyldipyrromethane is a superior tactic to the separation of a mixture of porphyrins, given the typical limited solubility and separability of porphyrin compounds.

Diacyldipyrromethane **2** was reduced by $NaBH_4$ to give the corresponding dipyrromethane-dicarbinol (**2-diol**). Condensation[60,61] of the latter with 5-(ethoxycarbonyl)dipyrromethane (**3**)[62] followed by oxidation afforded 3-bromo-15-ethoxycarbonyl-10,20-di-*p*-tolylporphyrin (**H_2P2-Br**) in 14% yield. Laser desorption mass spectrometry (LD-MS) analysis[63] of the crude mixture did not reveal any scrambling. Stille coupling of **H_2P2-Br** with hydroxymethyltributyltin (**4**),[64–67] as done previously with synthetic porphyrins[51] and chlorins,[68] yielded β-hydroxymethylporphyrin **H_2P2-OH** in 19% yield. Metalation of **H_2P2-OH** with $Zn(OAc)_2\cdot 2H_2O$ gave the corresponding zinc porphyrin in 95% yield.

Compound **ZnP2-OH** has a substitution pattern similar to the previously reported **ZnP1-OH** but lacks the linear

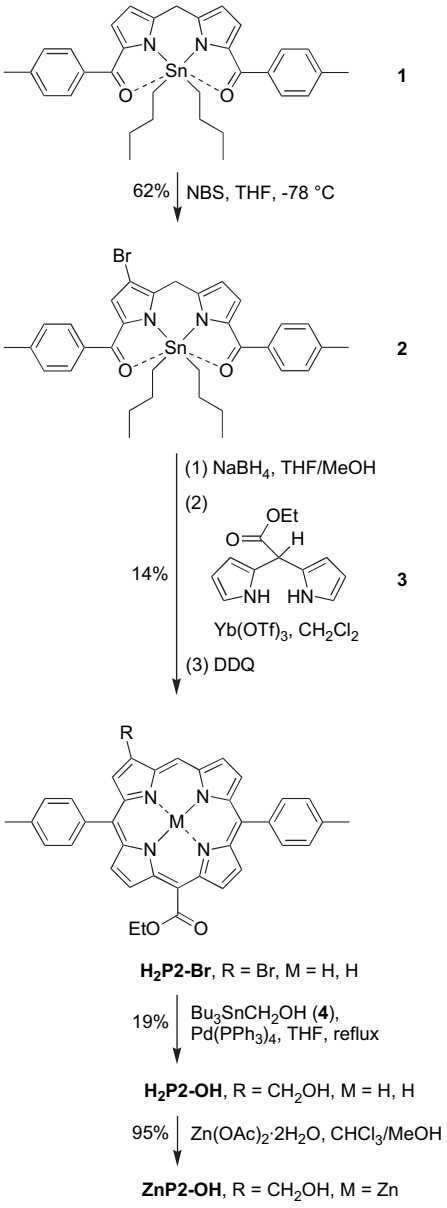

Scheme 1.

alignment of the three elements due to the hydroxymethyl group being at the β-position. Compound **ZnP2-OH** is soluble in CH_2Cl_2 with heating whereas the free base porphyrin **H_2P2-OH** is soluble in CH_2Cl_2 at room temperature. The β-hydroxymethylporphyrin was characterized by NMR (^{1}H, ^{13}C) spectroscopy, mass spectrometry, and absorption spectroscopy. The chemical shift of the hydroxy proton in **H_2P2-OH** is exceptionally low (2.38 ppm) versus the 5.14–6.31 ppm range for analogous *meso*-hydroxymethylporphyrins.[51]

2.2. Crystal structures

A sample of **ZnP1-OH** was crystallized from THF upon slow vapor diffusion of methanol. A sample of **ZnP2-OH** was crystallized from THF/acetone upon slow vapor diffusion of cyclohexane, or inadvertently from acetone-d_6/dimethylsulfoxide-d_6/THF (derived from an NMR sample); the two crystals of **ZnP2-OH** were found by X-ray

crystallography to be isostructural, with the solvent molecules occupying sites in both lattices. Only the former data are described herein. The X-ray analysis of **ZnP1-OH** exhibits bond distances and bond angles typical for a zinc porphyrin (Fig. 2a), as does that of **ZnP2-OH** (Fig. 2b).[69,70] The structural parameters for **ZnP1-OH** and **ZnP2-OH** and details for the X-ray analyses are shown in Table 1. The bond lengths and angles for **ZnP1-OH** and **ZnP2-OH** are unremarkable; however, the issues here concern the cell-packing pattern, and thus the overall assembled architecture of the molecules, rather than the molecular structure of the porphyrin macrocycle per se. These features are described below.

2.2.1. Crystal packing arrangement of ZnP1-OH. The dominant organization of the porphyrins in the crystal entails coordination polymers, wherein the carbonyl oxygen of the *meso* ester group on one porphyrin coordinates with the zinc ion on an adjacent porphyrin. The coordination of the ester group of one porphyrin to the apical zinc site of the adjacent porphyrin results in a staircase architecture for each polymer wherein the porphyrins in adjacent steps are cofacially offset. A given coordination polymer of apical-ligated porphyrins is present alongside a second polymer with essentially antiparallel macrocycle planes. The two polymers thus constitute a side-by-side or double staircase wherein the ester moieties of the individual porphyrin rings are thrust into a tract that runs down the middle of the two staircases (Fig. 3). Accordingly, the hydroxymethyl groups are positioned in tracts that run down the outer edges of the double staircase. The overall packing motif is composed of a pattern of such double staircases where the angle between double staircases is ~80°. The tract of hydroxymethyl groups on the edge of a given double staircase (composed of two coordination polymers) is juxtaposed with the hydroxymethyl groups of a nearly perpendicular double staircase.

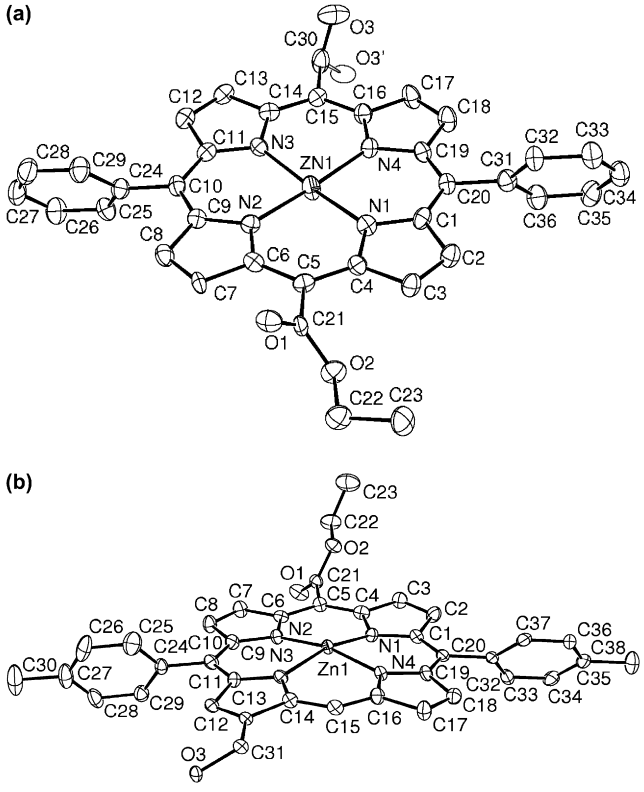

Figure 2. The ORTEP diagram with atom labeling for (a) **ZnP1-OH** and (b) **ZnP2-OH**. The thermal ellipsoids are drawn at the 50% probability level. Hydrogen atoms are omitted for clarity.

The specific intermolecular interactions between neighboring porphyrins include an O1(carbonyl oxygen)···Zn′ distance of 2.297 Å, and displacement of the zinc atom from the plane of the macrocycle toward the carbonyl oxygen by 0.114 Å. Although the apical coordination of the ester carbonyl group is clearly displayed, the hydroxy group at the *meso*-position trans to the ester group is orientationally disordered. When a given hydroxy group is pointed toward the zinc atom, the nearest hydroxy group from the adjacent double staircase forms a hydrogen bond with the hydroxy group coordinated to zinc. The O3(hydroxy oxygen)···Zn′ distance, when the hydroxy group is pointing toward the adjacent zinc atom, is 2.518 Å. Alternatively, a hydroxy group engages in hydrogen bonding along the tract between double staircases, as illustrated in Figure 4. The O3–H···O3 distance when participating in the O–H···O hydrogen bond along the tract is 1.981 Å, which is well within the range of known hydrogen bonds.[71] Thus, hydrogen bonding may exist between hydroxy groups in two adjacent double staircases, or the hydroxy group may be coordinated to the zinc atom of a porphyrin in the same staircase.

In the case where the hydroxy group is coordinated to the zinc atom of a porphyrin in the same staircase, the zinc atom is six-coordinate rather than five-coordinate (Fig. 5). The occupation for the oxygen atom (O3′) participating in such interactions is 0.43 and 0.57 for zinc coordination versus hydrogen bonding in the tract between double staircases, respectively. In summary, the hydroxy group disorder is driven by competition between multiple roles: OH···O hydrogen bonding versus HO···Zn apical coordination. The relative preference for one role versus the other depends on the energetics of the respective interactions. This feature highlights some of the subtleties in the design of crystalline molecular architectures.

The two adjacent macrocycles are slipped from a completely cofacial alignment to give only partial overlap of the π clouds (Fig. 6). The distance along the normal between the mean planes of two porphyrins in a coordination polymer is 3.36 Å. A given macrocycle is translated by 5.27 Å from the completely cofacial (i.e., coaxial) arrangement along the axis that bisects the 5,15-carbons (bearing the hydroxymethyl and ester groups). The macrocycle also is shifted by 0.69 Å along the axis that goes through the 10,20-carbons (bearing the phenyl groups). The resulting translation is such that the normal to the mean plane of the porphyrin forms an angle with the long axis of the coordination polymer of 57.6 and 10.4° along the 5,15- and 10,20-axis, respectively. Such a positioning places the carbonyl oxygen nearly directly above the zinc ion on the other porphyrin for apical coordination. The carbonyl group forms a dihedral angle of 45.40° with the macrocycle mean plane.

2.2.2. Crystal packing arrangement of ZnP2-OH. The dominant mode of organization entails infinite polymers of porphyrins. By contrast with **ZnP1-OH**, the ester group is not involved in direct ligation to the apical zinc site. In

Table 1. Summary of crystal data for **ZnP1-OH** and for **ZnP2-OH**

	ZnP1-OH	**ZnP2-OH**
Formula	$C_{36.50}H_{28}N_4O_{3.50}Zn$	$C_{42}H_{38}N_4O_4Zn$
Formula weight ($g\,mol^{-1}$)	644.00	728.16
Crystal dimensions (mm)	0.18×0.06×0.02	0.40×0.08×0.06
Crystal color and habit	Dark red prism	Dark red prism
Crystal system	Orthorhombic	Orthorhombic
Space group	*Pbca*	$Pca2_1$
Temperature (K)	110	110
a (Å)	6.30680(10)	26.0623(6)
b (Å)	28.5531(6)	10.1580(3)
c (Å)	31.8450(6)	13.1579(3)
α (°)	90.00	90.0
β (°)	90.00	90.0
γ (°)	90.00	90.0
V (Å^3)	5734.61(19)	3483.43(15)
Number of reflections to determine final unit cell	9973	9088
Min and max 2θ for cell determination (°)	4.78, 49.74	4.4, 48.8
Z	8	4
$F(000)$	2664	1522.09
ρ ($g\,cm^{-1}$)	1.492	1.388
λ (Å, Mo Kα)	0.71070	0.71073
μ (cm^{-1})	0.905	0.76
Diffractometer type	Bruker-Nonius X8 Apex2	Bruker-Nonius X8 Apex2
Scan type(s)	ϕ and ω Scans	ϕ and ω Scans
Max 2θ for data collection (°)	50.14	49.08
Measured fraction of data	0.999	1.00
Number of reflections measured	56,675	59,785
Unique reflections measured	5097	5795
R_{merge}	0.1103	0.034
Number of reflections included in refinement	5097	5423
Cut off threshold expression	$>2\sigma(I)$	$I_{net}>1.0\sigma(I_{net})$
Structure refined using	Full matrix least-squares using F^2	Full matrix least-squares using F
Weighting scheme	Calc $w=1/[\sigma^2(F_o^2)+(0.0570P)^2+40.8191P]$ where $P=(F_o^2+2F_c^2)/3$	$1/(\sigma^2(F)+0.0003F^2)$
Number of parameters in least-squares	430	461
R conventional	0.0746[a]	0.035[a]
R weighted	0.1778[b]	0.037[c]
R conventional (all data)	0.1170[a]	0.041[a]
R weighted (all data)	0.1989[b]	0.037[c]
GOF	1.085[d]	1.37[e]
Maximum shift/error	0.000	0.000
Min and max peak heights on final ΔF map (e^-/Å)	−0.575, 0.883	−0.38, 0.76

[a] R conventional $=\sum(|F_o|-|F_c|)/\sum|F_o|$.
[b] R weighted $=[\sum(w(F_o^2-F_c^2)^2)/\sum(wF_o^4)]^{1/2}$.
[c] R weighted $=[\sum(w(F_o^2-F_c^2)^2)/\sum F_o^2]^{1/2}$.
[d] GOF $=[\sum(w(F_o^2-F_c^2)^2)/(\text{No. of reflections}-\text{No. of parameters})]^{1/2}$.
[e] GOF $=[\sum(w(F_o-F_c)^2)/(\text{No. of reflections}-\text{No. of parameters})]^{1/2}$.

ZnP2-OH, the coordination of the hydroxymethyl group to the apical zinc site of the adjacent porphyrin results in a staircase architecture for each polymer wherein the porphyrins in adjacent steps are cofacially offset. The two coordination polymers run alongside each other, although the planes of the porphyrins in the respective polymers are not parallel but instead form an angle of 111° with respect to each other (Figs. 7 and 8). The lateral orientation of the porphyrins alternates with each step; thus, porphyrins 1, 3, 5, 7, etc. are positioned with the esters thrust to one side, and porphyrins 2, 4, 6, 8, etc. are positioned with the esters thrust to the opposite side. Consequently, each porphyrin polymer presents the ester moieties at the outer edges of the staircase, and on a given side every other porphyrin displays an outwardly thrust ester group.

The 'ester edge' of one porphyrin staircase interdigitates between alternating layers of the adjacent porphyrin staircase. Each ester of a given porphyrin is thus thrust toward a hydroxymethyl moiety of a porphyrin in an adjacent staircase. Such adjacent polymers are held by weak hydrogen bonds between the pyrrolic C–H and the oxygen atom from the ester group (C–H···O=C distance is 2.512 Å). Hydrogen bonds also exist between the hydroxy hydrogen of the porphyrin and the ethereal oxygen of the THF solvate (one molecule of THF per molecule of porphyrin). Because of the alternating staircase wherein adjacent porphyrins in a given staircase are offset and the esters are positioned on opposite (i.e., left or right) sides, the hydrogen bonds (esters to pyrrolic C–H) alternate between the two adjacent staircases. In other words, when the ester group of a given porphyrin forms

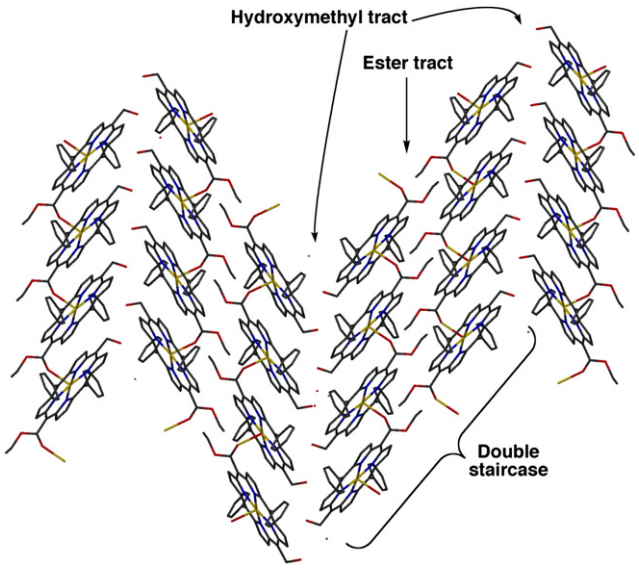

Figure 3. Packing arrangement showing a section of infinite coordination polymers of **ZnP1-OH**. The carbonyl oxygen of one porphyrin ligates to the apical zinc site of a second porphyrin. Two adjacent polymers form a double staircase containing an inner tract of ester moieties and outer tracts of hydroxymethyl groups. Note: the hydroxy groups in the crystal structure are disordered, and only one conformation is shown in the figure.

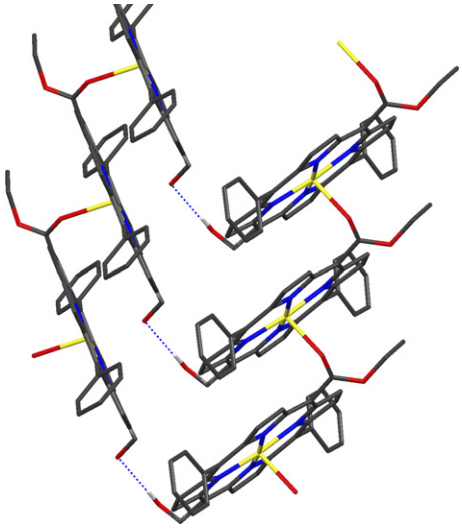

Figure 4. Possible hydrogen bonding between double staircases of **ZnP1-OH**. Note: the hydroxy groups in the crystal structure are disordered, and only one conformation is shown in the figure.

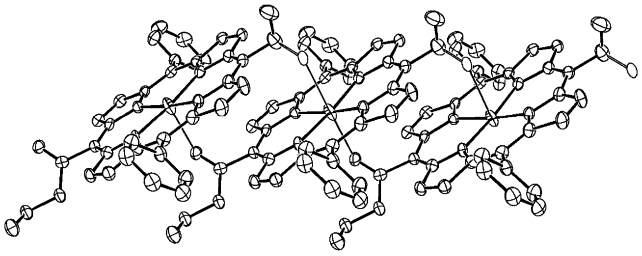

Figure 5. ORTEP drawing of **ZnP1-OH** showing the polymeric staircase stacking with hexa-coordinate zinc ions. Ellipsoids are at the 50% probability level and hydrogen atoms were omitted for clarity. The disordered O3′ position is shown as an open ellipsoid. All other atoms have principal axes drawn.

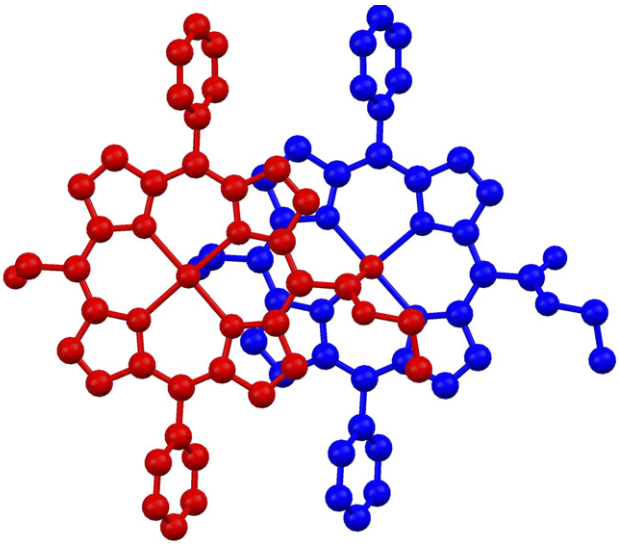

Figure 6. The top view of a portion of the infinite polymer of **ZnP1-OH** showing the partial cofacial overlap between two adjacent porphyrins.

a hydrogen bond with the 'left' adjacent polymer, the next one from the same polymer is bound to the 'right' adjacent polymer. Such arrangement defines a two-dimensional, infinite sheet of co-aligned coordination polymers wherein each polymer is held to two others by weak hydrogen bonding.

The molecular interactions between porphyrins in a coordination polymer are given in Figure 9. The Zn′–O1(hydroxy) distance is 2.177 Å, and the zinc atom is displaced from the mean macrocycle plane by 0.329 Å toward the apical oxygen atom. The zinc atom is five-coordinate. On the basis of the Zn–apical oxygen distances and the displacement of the Zn atom from the molecular plane, it appears that the Zn–OH interaction is much stronger than the Zn–carbonyl interaction in **ZnP1-OH**. The porphyrin mean planes of adjacent molecules in each stack are no longer parallel but exhibit a dihedral angle of 12°. Note that although the planes of adjacent porphyrins are not parallel, the planes of every other porphyrin are parallel. The distance between the mean planes of two parallel porphyrins is 7.330 Å. The neighboring porphyrin molecules are 'twisted' from the parallel orientation, with the angle between C10–C20 axes of two adjacent porphyrins of 150°. Such twisting positions the hydroxy oxygen nearly above the zinc atom of the next porphyrin. Consequently, the π-electron clouds of the macrocycles are only partially overlapped.

3. Outlook

The dominant structural motifs in the crystal lattices of both hydroxymethyl/ester-porphyrins are infinite coordination polymers. However, there are fundamental differences in the molecular interactions and the packing patterns of the two porphyrins. **ZnP1-OH** forms infinite polymers wherein the carbonyl oxygen of one porphyrin is ligated to the apical zinc site of the next porphyrin. The hydroxymethyl group is orientationally disordered: about half the molecules exhibit coordination of the hydroxy oxygen to the zinc site. A pair of such polymers forms a double staircase wherein the ethyl

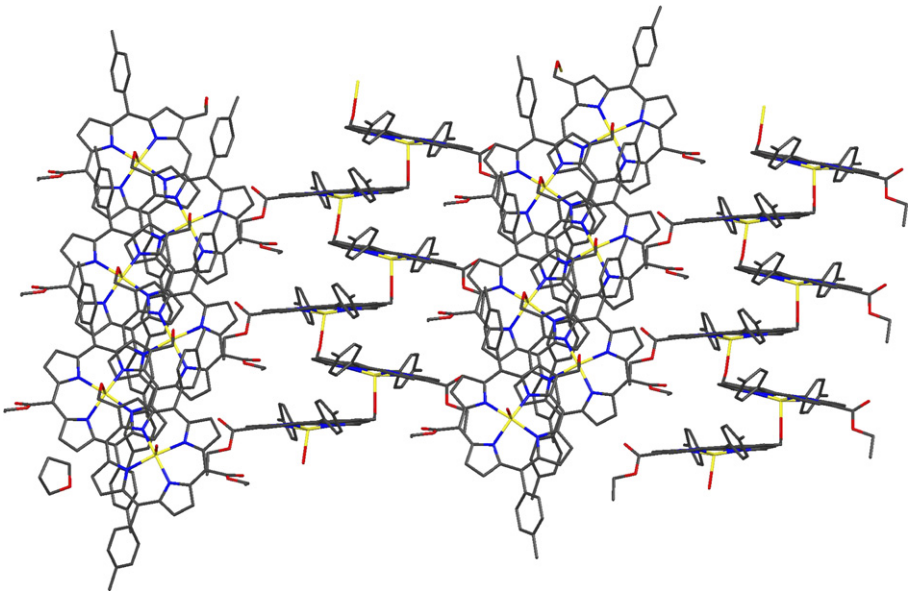

Figure 7. Packing arrangement of **ZnP2-OH**. The hydroxy oxygen of one porphyrin is ligated to the apical zinc site of a second porphyrin, yielding a staircase architecture wherein adjacent porphyrins are rotated and cofacially offset, and alternating porphyrins have parallel planes. The ester groups are not directly engaged in apical coordination to zinc, but interdigitate with the two adjacent polymers.

moieties form an inner tract between the polymers, and outer tracts of hydroxymethyl groups are positioned between adjoining double staircase. By contrast, **ZnP2-OH** forms infinite polymers wherein the hydroxymethyl group of one porphyrin is ligated to the apical zinc site of the next porphyrin, and the ester group is not directly coordinated to the zinc site. The neighboring porphyrin rings within each polymer are no longer parallel, and porphyrin axes are twisted by ~150°; however, alternating porphyrin rings exhibit mean planes that are essentially parallel. The two compounds also differ in the nature of the substituents at the flanking *meso*-positions (phenyl vs *p*-tolyl groups), but such groups are not expected to be the source of the fundamental differences in packing patterns.

The crystal structures exhibited by **ZnP1-OH** and **ZnP2-OH** can be compared with that for Balaban's porphyrin **I**, which bears a 5-α-hydroxyethyl group, a 15-acetyl group, and 10,20-bis(3,5-di-*tert*-butylphenyl) groups.[45] In the latter, an infinite polymer was observed wherein each zinc coordinated by a hydroxy group from one porphyrin and

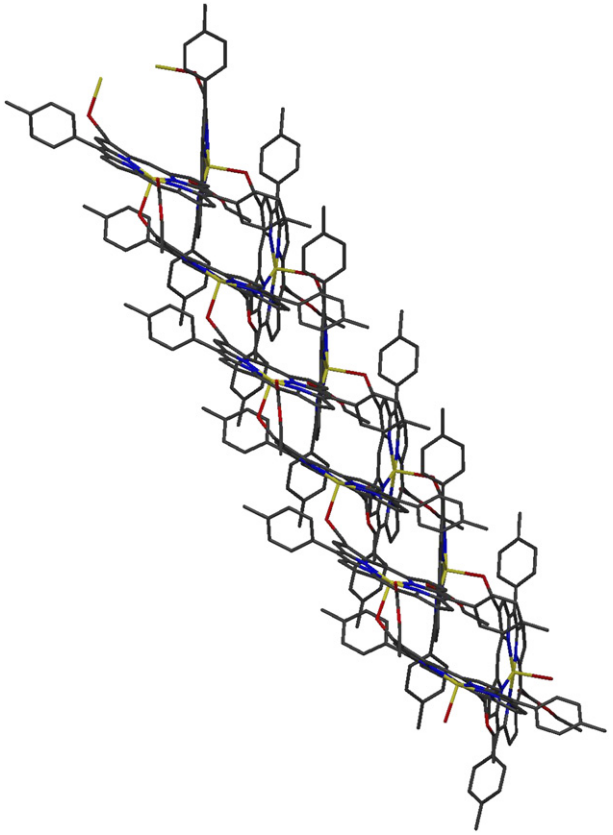

Figure 8. Packing arrangement of **ZnP2-OH**. Side view showing the staircase architecture of each of two polymers. Solvent molecules are omitted for clarity.

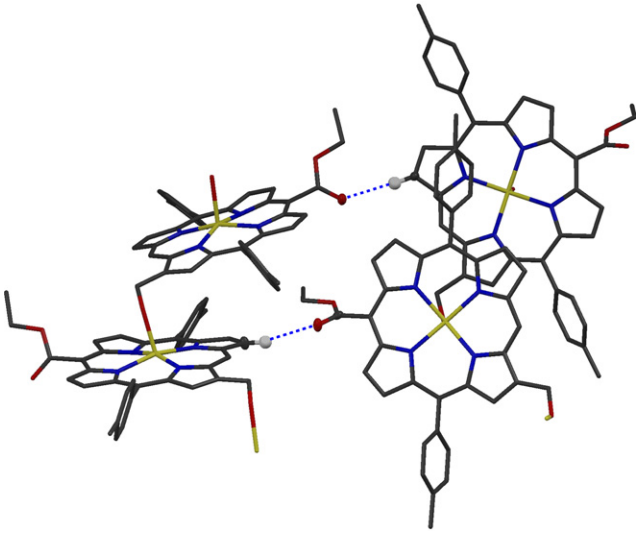

Figure 9. View of possible hydrogen bonding between porphyrins from two adjacent coordination polymers of **ZnP2-OH**.

(weakly) by a carbonyl group from a second porphyrin. The infinite polymer exhibited a staircase architecture with parallel porphyrin planes and offset cofacial overlap.

In all three cases (**ZnP1-OH**, **ZnP2-OH**, **I**), hydrogen bonding between hydroxy groups and carbonyl groups was not observed. Closed dimers also were not observed. The crystal structures are different from those of naturally occurring bacteriochlorophyll *c*, where the keto group is coplanar with the macrocycle. Thus, the observed crystal structures of porphyrins **ZnP1-OH**, **ZnP2-OH**, and **I** are each different from the model proposed for the assembly of bacteriochlorophyll *c* in chlorosomes. In all of the synthetic compounds, a significant unknown concerns the energy-transfer efficiency of the self-assembled crystalline architectures. The ability to synthesize diverse architectures should enable a broad study of the relationship between molecular structure, crystalline assembly, and excited-state energy-transfer processes. A deep understanding of this topic is critical to the development of functional light-harvesting architectures derived from self-assembling crystalline materials.

4. Experimental section

4.1. General methods

All ^{1}H NMR spectra (400 MHz) and ^{13}C NMR spectra (100 MHz) were recorded in $CDCl_3$ unless noted otherwise. Mass spectra of porphyrins were obtained by high-resolution fast atom bombardment mass spectrometry (FABMS) or by LD-MS.[63] Absorption spectra were collected in CH_2Cl_2 at room temperature unless noted otherwise. Melting points are uncorrected. Silica gel (40 μm average particle size) and alumina (80–200 mesh) were used for column chromatography. All reagents were used as received. Dry THF was distilled over Na/benzophenone.

4.2. Noncommercial compounds

Porphyrin **ZnP1-OH**;[51] dibutyltin complex of 1,9-diacyldipyrromethane **1**;[58] dipyrromethane **3**;[62] and tin reagent **4**[64–67] were prepared as described in the literature.

4.3. Synthetic procedures

4.3.1. Dibutyl-(3-bromo-5,10-dihydro-1,9-di-*p*-toluoyldipyrrinato)tin(IV) (2). Following a literature procedure for bromination of 1-acyldipyrromethanes,[57] a solution of **1** (10.8 g, 17.0 mmol) in dry THF (75 mL) at −78 °C under argon was treated with 1 mol equiv of NBS (3.10 g, 17.0 mmol) in one portion. The reaction mixture was stirred for 1 h at −78 °C. Hexanes/H_2O (1:1) was added, and the mixture was allowed to warm to room temperature. The organic layer was washed with H_2O, dried (K_2CO_3), and concentrated. Chromatography (silica, CH_2Cl_2 dried over K_2CO_3) yielded the dibromo product, the target mono-bromo product, and unreacted starting material. The title compound was obtained as a yellow solid (7.3 g, 62%). Mp 139–140 °C; ^{1}H NMR δ 0.70 (t, J=6.85 Hz, 6H), 1.10–1.20 (m, 5H), 1.30–1.39 (m, 5H), 1.50–1.60 (m, 2H), 2.45 (s, 6H), 4.30 (s, 2H), 6.41 (d, J=4.0 Hz, 1H), 7.17–7.18 (m, 2H), 7.31 (d, J=8.0 Hz, 4H), 7.78–7.87 (m, 4H); ^{13}C NMR δ 13.8, 21.9 (methyl carbons on the *p*-toluoyl groups overlapped), 24.6, 26.3, 27.1, 27.4, 100.5, 114.7, 124.09, 124.15, 129.28, 129.35 (two of the four signals for C2/C3 of *p*-toluoyl groups overlapped), 129.40, 134.3, 134.8, 134.9, 135.8, 142.6, 142.8, 144.3, 147.2, 184.2, 184.4. Anal. Calcd for $C_{33}H_{37}BrN_2O_2Sn$: C, 57.03; H, 5.39; N, 3.95. Found: C, 57.25; H, 5.39; N, 4.05.

4.3.2. 3-Bromo-15-(ethoxycarbonyl)-10,20-di-*p*-tolylporphyrin (H_2P2-Br). Following a literature procedure[60,61] with modifications, a solution of **2** (286 mg, 413 μmol) in dry THF/MeOH (10:1, 16 mL) was treated with $NaBH_4$ (310 mg, 8.20 mmol) for 2 h. Saturated aqueous NH_4Cl and CH_2Cl_2 were added. The organic layer was separated, dried (Na_2SO_4), and concentrated. The resulting dipyrromethane-dicarbinol and **3** (89.5 mg, 411 μmol) were dissolved in CH_2Cl_2 (170 mL). The mixture was treated with $Yb(OTf)_3$ (341 mg, 550 μmol) under argon for 30 min. DDQ (279 mg, 1.23 mmol) was added. The mixture was stirred for 30 min. TEA was added. The reaction mixture was concentrated. Chromatography [silica, hexanes/CH_2Cl_2 (1:4)] yielded a purple solid (36 mg, 14%). ^{1}H NMR δ −3.07 (br, 2H), 1.78 (t, J=6.8 Hz, 3H), 2.73 (s, 6H), 5.08 (q, J=7.1 Hz, 2H), 7.60 (d, J=7.6 Hz, 4H), 8.06–8.11 (m, 4H), 8.94 (s, 1H), 8.95 (d, J=4.8 Hz, 1H), 9.09 (d, J=4.8 Hz, 1H), 9.10 (d, J=4.8 Hz, 1H), 9.32 (d, J=5.2 Hz, 1H), 9.46 (d, J=4.8 Hz, 1H), 9.51 (d, J=5.2 Hz, 1H), 10.44 (s, 1H); ^{13}C NMR δ 15.0, 21.7, 63.3, 104.8, 110.3, 120.6, 121.1, 124.0, 127.7, 128.0, 128.0, 129.2, 129.6, 130.2, 132.9, 134.2, 134.8, 134.9, 135.1, 138.0, 138.2, 138.4, 138.5, 138.6, 139.0, 140.5, 141.6, 148.5, 151.6, 152.7, 154.7, 171.7; LD-MS obsd 640.3; FABMS obsd 640.1470, calcd 640.1474 ($C_{37}H_{29}BrN_4O_2$); λ_{abs} 415, 511, 583, 638 nm.

4.3.3. 15-(Ethoxycarbonyl)-3-hydroxymethyl-10,20-di-*p*-tolylporphyrin (H_2P2-OH). Following a standard procedure,[51,68] a mixture of **H_2P2-Br** (55 mg, 80 μmol), hydroxymethyltributyltin (**4**, 42 mg, 0.13 mmol), and $Pd(PPh_3)_4$ (10 mg, 8.0 μmol) was refluxed in THF (2.5 mL) for 48 h in a Schlenk flask. The crude mixture was concentrated. Chromatography (silica, CH_2Cl_2) yielded a purple solid (9.0 mg, 19%). ^{1}H NMR δ −3.08 (br, 2H), 1.78 (t, J=7.2 Hz, 3H), 2.34–2.39 (m, 1H), 2.73 (s, 6H), 2.87 (br, 1H), 5.08 (q, J=6.8 Hz, 2H), 6.11–6.17 (m, 2H), 7.57–7.62 (m, 4H), 8.07 (d, J=8.0 Hz, 2H), 8.10 (d, J=7.6 Hz, 2H), 8.89 (s, 1H), 9.01–9.03 (m, 3H), 9.33 (d, J=5.2 Hz, 1H), 9.41 (d, J=4.8 Hz, 1H), 9.44 (d, J=4.8 Hz, 1H), 10.35 (s, 1H); ^{13}C NMR δ 15.0, 21.7, 59.9, 63.3, 104.3, 120.5, 120.9, 127.9, 134.7, 134.8, 137.85, 137.88, 138.6, 171.9; LD-MS obsd 592.6; FABMS obsd 593.2552, calcd 593.2553 ($C_{38}H_{32}N_4O_3$); λ_{abs} 413, 510, 581 nm.

4.3.4. Zn(II)-15-(ethoxycarbonyl)-3-hydroxymethyl-10,20-di-*p*-tolylporphyrin (ZnP2-OH). A solution of **H_2P2-OH** (20.0 mg, 33.8 μmol) in CH_2Cl_2/MeOH (4:1, 10 mL) was treated with $Zn(OAc)_2$ (31.1 mg, 169 μmol) at room temperature for 30 min. The reaction mixture was concentrated. Chromatography [silica, CH_2Cl_2/ethyl acetate (19:1)] yielded a red-purple solid (21 mg, 95%). ^{1}H NMR δ (acetone-d_6) 1.75 (t, J=7.3 Hz, 3H), 2.73 (s, 6H), 4.83 (t, J=5.5 Hz, 1H), 5.06 (q, J=7.3 Hz, 2H), 6.05 (d, J=5.5 Hz,

2H), 7.62–7.67 (m, 4H), 8.06–8.14 (m, 3H), 8.83 (s, 1H), 8.96–9.02 (m, 3H), 9.43–9.48 (m, 3H), 10.4 (s, 1H); ^{13}C NMR δ 15.1, 21.58, 21.61, 59.5, 63.3, 105.9, 111.2, 121.2, 121.8, 128.2, 130.8, 130.9, 131.1, 135.3, 135.4, 138.0, 138.0, 141.0, 141.1, 147.2, 148.5, 148.58, 148.64, 150.3, 150.5, 150.8, 151.1, 151.4, 172.9; LD-MS obsd 654.9; FABMS obsd 654.1644, calcd 654.1609 ($C_{38}H_{30}N_4O_3Zn$); λ_{abs} 416, 545, 575, 656 nm.

4.3.5. Zn(II)-3-bromo-15-(ethoxycarbonyl)-10,20-di-*p*-tolylporphyrin (ZnP2-Br). A solution of **H_2P2-Br** (38.6 mg, 60.1 μmol) in $CHCl_3$/MeOH (22 mL, 10:1) was treated with $Zn(OAc)_2$ (55.0 mg, 301 μmol) at room temperature for 4 h. The reaction mixture was concentrated. Chromatography (silica, CH_2Cl_2) yielded a red-purple solid (41 mg, 98%). ^{1}H NMR δ 1.24 (t, J=8.0 Hz, 3H), 2.79 (s, 6H), 4.12 (q, J=7.5 Hz, 2H), 7.62 (d, J=7.5 Hz, 1H), 8.10–8.17 (m, 4H), 8.36–8.42 (m, 2H), 8.83–8.89 (m, 2H), 9.07–9.12 (m, 3H), 9.46 (d, J=4.5 Hz, 1H), 10.5 (s, 1H); LD-MS obsd 701.8; FABMS obsd 702.0661, calcd 702.0609 ($C_{37}H_{27}BrN_4O_2Zn$); λ_{abs} 416, 544, 574, 656 nm.

4.3.6. Alternative preparation of ZnP2-OH. A mixture of **ZnP2-Br** (41.3 mg, 58.7 μmol), $(PPh_3)_4Pd$ (6.79 mg, 5.87 μmol), and hydroxymethyltributyltin (**4**, 20.7 mg, 64.6 μmol) was refluxed in THF (4 mL) in a Schlenk flask for 18 h. The mixture was concentrated. Chromatography [silica, CH_2Cl_2/ethyl acetate (19:1)] yielded a red-purple solid (21.3 mg, 55%). The characterization data were consistent with those described above.

4.4. X-ray crystallographic analysis

4.4.1. Data collection and processing. The samples were mounted on a nylon loop with a small amount of NVH immersion oil. All X-ray measurements were made on a Bruker-Nonius X8 Apex2 CCD diffractometer at 110 K. The frame integration was performed using SAINT+.[72] The resulting raw data were scaled and absorption-corrected by multi-scan averaging of symmetry equivalent data using SADABS.[73]

4.4.2. Structure solution and refinement. The structures were solved by direct methods using SIR92.[74] All non-hydrogen atoms were obtained from the initial E-map. The hydrogen atom positions were placed at idealized positions and were allowed to ride on the parent carbon atom. The structural model was fit to the data using full matrix least-squares based on F^2 (for **ZnP1-OH**) or F (for **ZnP2-OH**). The calculated structural factors included corrections for anomalous dispersion from the usual tabulation. The structure was refined using the XL program from the SHELXTL package.[75] Graphic plots were produced using the version of ORTEP included in the NRCVAX crystallographic program suite.[76] Crystallographic data for the structures **ZnP1-OH** and **ZnP2-OH** have been deposited with the Cambridge Crystallographic Data Centre as supplementary publication under numbers CCDC 662534 and CCDC 662755. Copies of the data can be obtained, free of charge, on application to CCDC, 12 Union Road, Cambridge CB2 1EZ, UK (fax:+44-(0)1223-336033 or e-mail: deposit@ccdc.cam.ac.uk).

Acknowledgements

This work was supported by a grant from the Division of Chemical Sciences, Office of Basic Energy Sciences, Office of Energy Research, U.S. Department of Energy (DE-FG02-96ER14632). Mass spectra were obtained at the Mass Spectrometry Laboratory for Biotechnology at North Carolina State University. Partial funding for the Facility was obtained from the North Carolina Biotechnology Center and the National Science Foundation. The Department of Chemistry of North Carolina State University and the State of North Carolina provided funds to purchase the Apex2 diffractometer.

References and notes

1. Green, B. R.; Anderson, J. M.; Parson, W. W. *Light-Harvesting Antennas in Photosynthesis*; Green, B. R., Parson, W. W., Eds.; Kluwer Academic: The Netherlands, 2003; pp 1–28.
2. Blankenship, R. E.; Olson, J. M.; Miller, M. *Anoxygenic Photosynthetic Bacteria*; Blankenship, R. E., Madigan, M. T., Bauer, C. E., Eds.; Kluwer Academic: The Netherlands, 1995; pp 399–435.
3. Scheer, H. *Chlorophylls and Bacteriochlorophylls: Biochemistry, Biophysics, Functions and Applications*; Grimm, B., Porra, R. J., Rüdiger, W., Scheer, H., Eds.; Kluwer Academic: The Netherlands, 2006; pp 1–26.
4. Tamiaki, H. *Coord. Chem. Rev.* **1996**, *148*, 183–197.
5. Tamiaki, H.; Holzwarth, A. R.; Schaffner, K. *J. Photochem. Photobiol., B: Biol.* **1992**, *15*, 355–360.
6. Tamiaki, H.; Takeuchi, S.; Tanikaga, R.; Balaban, S. T.; Holzwarth, A. R.; Schaffner, K. *Chem. Lett.* **1994**, 401–402.
7. Tamiaki, H.; Holzwarth, A. R.; Schaffner, K. *Photosynth. Res.* **1994**, *41*, 245–251.
8. Tamiaki, H.; Miyata, S.; Kureishi, Y.; Tanikaga, R. *Tetrahedron* **1996**, *52*, 12421–12432.
9. Tamiaki, H.; Kubota, T.; Tanikaga, R. *Chem. Lett.* **1996**, *8*, 639–640.
10. Tamiaki, H.; Amakawa, M.; Shimono, Y.; Tanikaga, R.; Holzwarth, A. R.; Schaffner, K. *Photochem. Photobiol.* **1996**, *63*, 92–99.
11. Tamiaki, H.; Miyatake, T.; Tanikaga, R.; Holzwarth, A. R.; Schaffner, K. *Angew. Chem., Int. Ed.* **1996**, *35*, 772–774.
12. Tamiaki, H.; Miyatake, T.; Tanikaga, R. *Tetrahedron Lett.* **1997**, *38*, 267–270.
13. Tamiaki, H.; Kouraba, M. *Tetrahedron* **1997**, *53*, 10677–10688.
14. Balaban, T. S.; Tamiaki, H.; Holzwarth, A. R.; Schaffner, K. *J. Phys. Chem. B* **1997**, *101*, 3424–3431.
15. Oba, T.; Furukawa, H.; Wang, Z.-Y.; Nozawa, T.; Mimuro, M.; Tamiaki, H.; Watanabe, T. *J. Phys. Chem. B* **1998**, *102*, 7882–7889.
16. Tamiaki, H.; Takeuchi, S.; Tsudzuki, S.; Miyatake, T.; Tanikaga, R. *Tetrahedron* **1998**, *54*, 6699–6718.
17. Kureishi, Y.; Tamiaki, H. *J. Porphyrins Phthalocyanines* **1998**, *2*, 159–169.
18. Oba, T.; Tamiaki, H. *Photochem. Photobiol.* **1998**, *67*, 295–303.
19. Oba, T.; Tamiaki, H. In: *Photosynthesis: Mechanisms and Effects*, Proceedings of the International Congress on Photosynthesis, 11th, Budapest, Aug. 17–22, 1998; Garab, G., Ed.; Kluwer Academic: Netherlands, 1998; Vol. 1, pp 465–468.
20. Miyatake, T.; Tamiaki, H.; Holzwarth, A.R.; Schaffner, K. In: *Photosynthesis: Mechanisms and Effects*, Proceedings of the International Congress on Photosynthesis, 11th, Budapest,

Aug. 17–22, 1998; Garab, G., Ed.; Kluwer Academic: Netherlands, 1998; Vol. 1, pp 133–136
21. Yagai, S.; Miyatake, T.; Tamiaki, H. *J. Photochem. Photobiol., B: Biol.* **1999**, *52*, 74–85.
22. Oba, T.; Tamiaki, H. *Photosynth. Res.* **1999**, *61*, 23–31.
23. Miyatake, T.; Tamiaki, H.; Holzwarth, A. R.; Schaffner, K. *Photochem. Photobiol.* **1999**, *69*, 448–456.
24. Tamiaki, H.; Kubo, M.; Oba, T. *Tetrahedron* **2000**, *56*, 6245–6257.
25. Yagai, S.; Miyatake, T.; Shimono, Y.; Tamiaki, H. *Photochem. Photobiol.* **2001**, *73*, 153–163.
26. Yagai, S.; Tamiaki, H. *J. Chem. Soc., Perkin Trans. 1* **2001**, 3135–3144.
27. Miyatake, T.; Oba, T.; Tamiaki, H. *ChemBioChem* **2001**, *2*, 335–342.
28. Yagai, S.; Miyatake, T.; Tamiaki, H. *J. Org. Chem.* **2002**, *67*, 49–58.
29. Tamiaki, H.; Amakawa, M.; Holzwarth, A. R.; Schaffner, K. *Photosynth. Res.* **2002**, *71*, 59–67.
30. Prokhorenko, V. I.; Holzwarth, A. R.; Müller, M. G.; Schaffner, K.; Miyatake, T.; Tamiaki, H. *J. Phys. Chem. B* **2002**, *106*, 5761–5768.
31. Miyatake, T.; Tamiaki, H.; Shinoda, H.; Fujiwara, M.; Matsushita, T. *Tetrahedron* **2002**, 9989–10000.
32. Tamiaki, H.; Omoda, M.; Saga, Y.; Morishita, H. *Tetrahedron* **2003**, *59*, 4337–4350.
33. Tamiaki, H.; Kimura, S.; Kimura, T. *Tetrahedron* **2003**, *59*, 7423–7435.
34. Sasaki, S.-i.; Omoda, M.; Tamiaki, H. *J. Photochem. Photobiol., A: Chem.* **2004**, *162*, 307–315.
35. Sasaki, S.-i.; Tamiaki, H. *Bull. Chem. Soc. Jpn.* **2004**, *77*, 797–800.
36. Kunieda, M.; Mizoguchi, K.; Tamiaki, H. *Photochem. Photobiol.* **2004**, *79*, 55–61.
37. de Boer, I.; Matysik, J.; Erkelens, K.; Sasaki, S.-i.; Miyatake, T.; Yagai, S.; Tamiaki, H.; Holzwarth, A. R.; de Groot, H. J. M. *J. Phys. Chem. B* **2004**, *108*, 16556–16566.
38. Tamiaki, H.; Kitamoto, H.; Nishikawa, A.; Hibino, T.; Shibata, R. *Bioorg. Med. Chem.* **2004**, *12*, 1657–1666.
39. Kunieda, M.; Tamiaki, H. *Eur. J. Org. Chem.* **2006**, 2352–2361.
40. Miyatake, T.; Tanigawa, S.; Kato, S.; Tamiaki, H. *Tetrahedron Lett.* **2007**, *48*, 2251–2254.
41. Kunieda, M.; Tamiaki, H. *J. Org. Chem.* **2007**, *72*, 2443–2451.
42. Balaban, T. S.; Eichhöfer, A.; Lehn, J.-M. *Eur. J. Org. Chem.* **2000**, 4047–4057.
43. Balaban, T. S.; Bhise, A. D.; Fischer, M.; Linke-Schaetzel, M.; Roussel, C.; Vanthuyne, N. *Angew. Chem., Int. Ed.* **2003**, *42*, 2140–2144.
44. Balaban, T. S.; Linke-Schaetzel, M.; Bhise, A. D.; Vanthuyne, N.; Roussel, C. *Eur. J. Org. Chem.* **2004**, 3919–3930.
45. Balaban, T. S.; Linke-Schaetzel, M.; Bhise, A. D.; Vanthuyne, N.; Roussel, C.; Anson, C. E.; Buth, G.; Eichhöfer, A.; Foster, K.; Garab, G.; Gliemann, H.; Goddard, R.; Javorfi, T.; Powell, A. K.; Rösner, H.; Schimmel, T. *Chem.—Eur. J.* **2005**, *11*, 2267–2275.
46. Balaban, T. S.; Tamiaki, H.; Holzwarth, A. R. *Top. Curr. Chem.* **2005**, *258*, 1–38.
47. Balaban, T. S. *Acc. Chem. Res.* **2005**, *38*, 612–623.
48. Miyatake, T.; Tamiaki, H. *J. Photochem. Photobiol., C: Photochem. Rev.* **2005**, *6*, 89–107.
49. Tamiaki, H.; Shibata, R.; Mizoguchi, T. *Photochem. Photobiol.* **2007**, *83*, 152–162.
50. Kobuke, Y. *Struct. Bonding* **2006**, *121*, 49–104.
51. Yao, Z.; Bhaumik, J.; Savithri, D.; Ptaszek, M.; Rodriguez, P.; Lindsey, J. S. *Tetrahedron* **2007**, *63*, 10657–10670.
52. Kamogawa, H.; Nakata, T.; Komatsu, S. *Bull. Chem. Soc. Jpn.* **1991**, *64*, 2300–2302.
53. Vicente, M. G. H. *The Porphyrin Handbook*; Kadish, K. M., Smith, K. M., Guilard, R., Eds.; Academic: San Diego, CA, 2000; Vol. 1, pp 149–199.
54. Jaquinod, L. *The Porphyrin Handbook*; Kadish, K. M., Smith, K. M., Guilard, R., Eds.; Academic: San Diego, CA, 2000; Vol. 1, pp 201–237.
55. Balasubramanian, T.; Lindsey, J. S. *Tetrahedron* **1999**, *55*, 6771–6784.
56. Balasubramanian, T.; Strachan, J.-P.; Boyle, P. D.; Lindsey, S. J. *J. Org. Chem.* **2000**, *65*, 7919–7929.
57. Liu, Z.; Yasseri, A. A.; Loewe, R. S.; Lysenko, A. B.; Malinovskii, V. L.; Zhao, Q.; Surthi, S.; Li, Q.; Misra, V.; Lindsey, J. S.; Bocian, D. F. *J. Org. Chem.* **2004**, *69*, 5568–5577.
58. Tamaru, S.-I.; Yu, L.; Youngblood, W. J.; Muthukumaran, K.; Taniguchi, M.; Lindsey, J. S. *J. Org. Chem.* **2004**, *69*, 765–777.
59. Lee, C.-H.; Li, F.; Iwamoto, K.; Dadok, J.; Bothner-By, A. A.; Lindsey, J. S. *Tetrahedron* **1995**, *51*, 11645–11672.
60. Rao, P. D.; Dhanalekshmi, S.; Littler, B. J.; Lindsey, J. S. *J. Org. Chem.* **2000**, *65*, 7323–7344.
61. Geier, G. R., III; Callinan, J. B.; Rao, P. D.; Lindsey, J. S. *J. Porphyrins Phthalocyanines* **2001**, *5*, 810–823.
62. Trova, M. P.; Gauuan, P. J. F.; Pechulis, A. D.; Bubb, S. M.; Bocckino, S. B.; Crapo, J. D.; Day, B. J. *Bioorg. Med. Chem.* **2003**, *11*, 2695–2707.
63. Srinivasan, N.; Haney, C. A.; Lindsey, J. S.; Zhang, W.; Chait, B. T. *J. Porphyrins Phthalocyanines* **1999**, *3*, 283–291.
64. Kosugi, M.; Sumiya, T.; Ogata, T.; Sano, H.; Migita, T. *Chem. Lett.* **1984**, 1225–1226.
65. Kosugi, M.; Sumiya, T.; Ohhashi, K.; Sano, H.; Migita, T. *Chem. Lett.* **1985**, 997–998.
66. Danheiser, R. L.; Romines, K. R.; Koyama, H.; Gee, S. K.; Johnson, C. R.; Medich, J. R. *Org. Synth.* **1993**, *71*, 133–139.
67. Åhman, J.; Somfai, P. *Synth. Commun.* **1994**, *24*, 1117–1120.
68. Muthiah, C.; Bhaumik, J.; Lindsey, J. S. *J. Org. Chem.* **2007**, *72*, 5839–5842.
69. Scheidt, W. R.; Lee, Y. J. *Structure and Bonding*; Buchler, J. W., Ed.; Springer: Berlin, 1987; Vol. 64, pp 1–70.
70. Senge, M. O. *The Porphyrin Handbook*; Kadish, K. M., Smith, K. M., Guilard, R., Eds.; Academic: San Diego, CA, 2000; Vol. 10, pp 1–218.
71. Desiraju, G. R. *Acc. Chem. Res.* **1991**, *24*, 290–296.
72. Bruker-Nonius. *SAINT+ version 7.07B*; Bruker-Nonius: Madison, WI, 2004.
73. Bruker-Nonius. *SADABS version 2.10*; Bruker-Nonius: Madison, WI, 2004.
74. Altomare, A.; Cascarano, G.; Giacovazzo, C.; Guagliardi, A.; Burla, M. C.; Polidori, G.; Camalli, M. *J. Appl. Crystallogr.* **1994**, *27*, 435.
75. *Bruker-AXS, XL, SHELXTL version 6.12, UNIX*; Bruker-Nonius: Madison, WI, 2001.
76. Gabe, E. J.; Le Page, Y.; Charland, J.-P.; Lee, F. L.; White, P. S. *J. Appl. Crystallogr.* **1989**, *22*, 384–387.